Available online at www.sciencedirect.com
ScienceDirect
Journal of the European Ceramic Society 27 (2007) 1345–1350
www.elsevier.com/locate/jeurceramsoc

Preparation and thermal conductivity characterisation of highly porous ceramics Comparison between experimental results, analytical calculations and numerical simulations

B. Nait-Ali [a], K. Haberko [b], H. Vesteghem [a], J. Absi [a,*], D.S. Smith [a]

[a] *Groupe d'Etude des Matériaux Hétérogènes, Ecole Nationale Supérieure de Céramique Industrielle, 47-73 Avenue Albert Thomas, 87065 Limoges Cedex, France*

[b] *University of Mining & Metallurgy, Faculty of Materials Science and Ceramics, Al. Mickiewicza 30, 30-059 Krakow, Poland*

Available online 2 June 2006

Abstract

Two sets of highly porous materials with different intrinsic thermal conductivity values for the solid skeleton were prepared: zirconia and alumina. Microstructural characterisation was performed, including the determination of the pore size distribution (PSD). The pore volume fraction was varied from 40 to 75%. Zirconia samples exhibit heterogeneous microstructures with a bimodal PSD. Alumina samples seems to be more organised with a monomodal PSD.

The effective thermal conductivity was evaluated using the laser-flash technique. The experimental values were compared with predictions made with analytical models as a function of porosity. In particular, effective medium percolation theory (EMPT) for a two-phase system gives calculated values which are close to the experimental results for zirconia samples when the bimodal PSD was taken into account. Measurements on alumina samples have shown that EMPT is of limited use for an organised microstructure with porosity exceeding 65%.

Complementary studies by computer simulation were also used to support some of the deductions which were made concerning the influence of the microstructure organisation on the effective thermal conductivity.

Keywords: Thermal conductivity; Porosity; ZrO_2; Al_2O_3

1. Introduction

Research towards a better understanding of the physical properties of heterogeneous solids has both scientific and technological importance. One particular class of these solids is constituted by materials containing a large volume fraction of porosity which are used in situations requiring very good thermal insulation.[1] The prediction of their thermal properties and especially the effective conductivity by analytical or computer calculation is therefore of strong interest.[2,3] Collishaw and Evans[4] have reviewed some analytical expressions for the calculation of the effective thermal conductivity of a porous solid. In each case, the expression is based on a geometrical simplification of the microstructure concerning the spatial distribution of the pore phase in the solid matrix. The pertinence of this approximation to the real microstructure determines the validity of a chosen model.

For materials containing small amounts of porosity (<20%), the prediction of the thermal conductivity is less critical than for highly porous materials. This study deals with the influence of the microstructure on the effective thermal conductivity for materials containing from 45 to 75% porosity through experimental measurements, analytical and computer calculations.

2. Experimental procedure

2.1. Sample preparation

2.1.1. Zirconia samples

Zirconia samples were prepared from a hydrothermally crystallized 8 mol% yttria stabilised zirconia (8-YSZ) suspension.[5] Crystallites of about 6 nm form agglomerates with a mean grain size of about 1 μm. The suspension was mixed with a

* Corresponding author.
E-mail address: j_absi@ensci.fr (J. Absi).

0955-2219/$ – see front matter © 2006 Elsevier Ltd. All rights reserved.
doi:10.1016/j.jeurceramsoc.2006.04.025

commercial latex (Rhoximat UP 600B, Rhodia) with a fixed volume ratio (polymer/zirconia). The mean particle size of the polymer depends on the dilution and its value is between 1 and 5 μm. After drying the mixture for 24 h at room temperature in order to form a paste, disk samples were uniaxially pressed at 100 MPa. The pore volume fraction was varied by adjusting the maximum sintering temperature.

2.1.2. Alumina samples

Porous alumina samples were prepared from a powder with a mean grain size of about 0.5 μm. This powder was mixed with a dry polymer (Rhoximat PSB 150, Rhodia). The mean particle size of the polymer is 80 μm. Disk samples were uniaxially pressed at 100 MPa and fired at 1400 °C for 6 min. The pore volume fraction was varied by modifying the following volume ratio: $v = V_{\text{polymer}}/(V_{\text{polymer}} + V_{\text{zirconia}})$.

2.2. Microstructure characterisation

The pore volume fraction in each sample was determined by the method based on Archimedes' principle. Our interest was then focused on the characterisation of the porous network. Samples were observed with the scanning electron microscope (SEM). These micrographs give information about grain sizes, pore shape and size. Mean grain sizes were determined using image analysis software. The pore size distributions in the samples were also evaluated using mercury porosimetry measurements.

2.3. Thermal conductivity measurement

The laser-flash method was used to determine, via the thermal diffusivity, the overall thermal conductivity of the samples. A short duration pulse (0.5 ms) of a laser beam (assimilated in theory to a Dirac function) is used to heat up the front face of the cylindrical sample. The absorbed heat diffuses throughout the sample and an infrared detector is used to monitor the evolution of the back face temperature. Degiovanni's[6] method, which takes into account heat losses, was used to calculate the thermal diffusivity (α) from an analysis of the back face temperature–time behaviour. The thermal conductivity (λ) is then obtained using Eq. (1):

$$\lambda = \alpha \rho c \tag{1}$$

where ρ is the density and c is the specific heat of the material. The specific heat was obtained from literature values which take into account the molar fraction of Y_2O_3 in the zirconia matrix.[7]

2.4. Prediction of the effective thermal conductivity

Analytical and also computer modelling require knowledge of the thermal conductivity of each phase. For the thermal conductivity of air (λ_{air}), a literature value equal to 0.026 W m^{-1} K^{-1} was used.[8] This value was eventually adjusted to take into account the pore size with the Knudsen effect for spherical pores.[4]

The thermal conductivity for the solid phase (λ_s) was determined from literature data. The value was adjusted to take into account the interfacial thermal resistance of the grain boundaries (R^*_{int}) according to Eq. (2):

$$\frac{1}{\lambda_{\text{poly}}} = \frac{1}{\lambda_{\text{single crystal}}} + n R^*_{\text{int}} \tag{2}$$

where $\lambda_{\text{single crystal}}$ and λ_{poly} are, respectively, the thermal conductivity of the single crystal and the polycrystalline material and n is the number of interfaces per unit length.

Values of average interfacial thermal resistance of a grain boundary were evaluated for 8-YSZ by Yang et al.[9] and for alumina by Smith et al.[10]

2.4.1. Analytical calculations

The experimental results were compared with two analytical models. First, the upper limit of Hashin and Shtrikman[11] (HS+) expressions for a two-phase system describes the thermal conductivity for isolated inclusions (pores) placed in a continuous matrix. Second, Landauer's[12] effective medium percolation theory (EMPT) predicts the thermal conductivity for a random mixture of two homogeneous phases.[13]

2.4.2. Computer modelling

Computer simulations, using finite element modelling (FEM) were also conducted to investigate the role of the microstructure on the effective thermal conductivity. This study is complementary to the work by Grandjean et al.[3] on porous ceramics with pore volume fraction less than 30%. The software package ABAQUS was used to calculate the heat conduction for the steady state. The thermal conductivity of each phase (solid and air) was taken into account. A temperature difference was imposed across the upper and lower boundaries of the geometrical model. The effective thermal conductivity was then calculated from the average heat flow across the lower boundary using Fourier's law. Different geometries were used to relate microstructural information of each sample. A software was developed using C++ language to generate complex microstructures. 3D geometrical models presented in Fig. 1 with open porosities were produced. First, the pores are randomly placed and the PSD could be monomodal (Fig. 1a) or bimodal (Fig. 1b). Second, organised 3D geometrical models based on spherical pores were generated (Fig. 1c).

3. Results and discussion

3.1. Sample characterisation

3.1.1. Zirconia samples

Pore volume fraction was varied from 45 to 75% by adjusting the maximum sintering temperature between 750 and 1100 °C.

The micrograph in Fig. 2a reveals a homogeneous grain size of less than 100 nm and variation in pore shape and size. At least two different characteristic pore sizes can be identified. The mercury porosimetry measurement in Fig. 2b confirms that the samples exhibit bimodal PSDs, constituted by mesopores

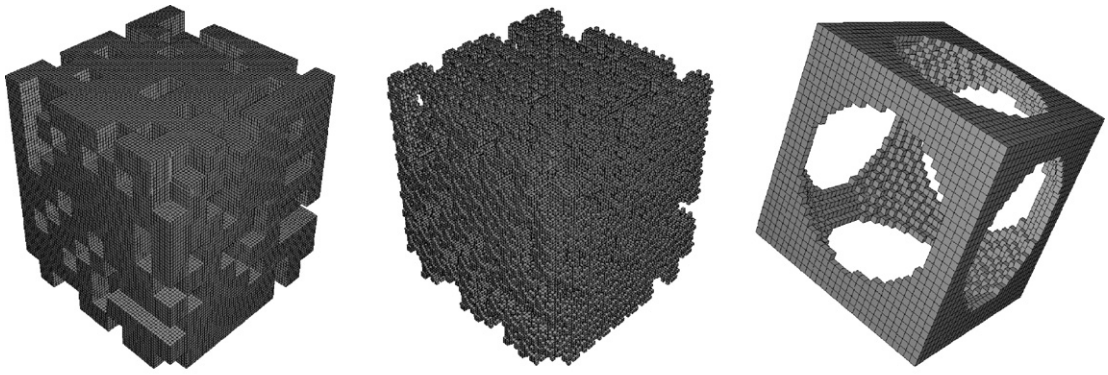

(a) (b) (c)

Fig. 1. 3D geometrical models. Random porosity with: (a) a monomodal PSD and (b) a bimodal PSD. (c) Organised microstructure based on a spherical pore.

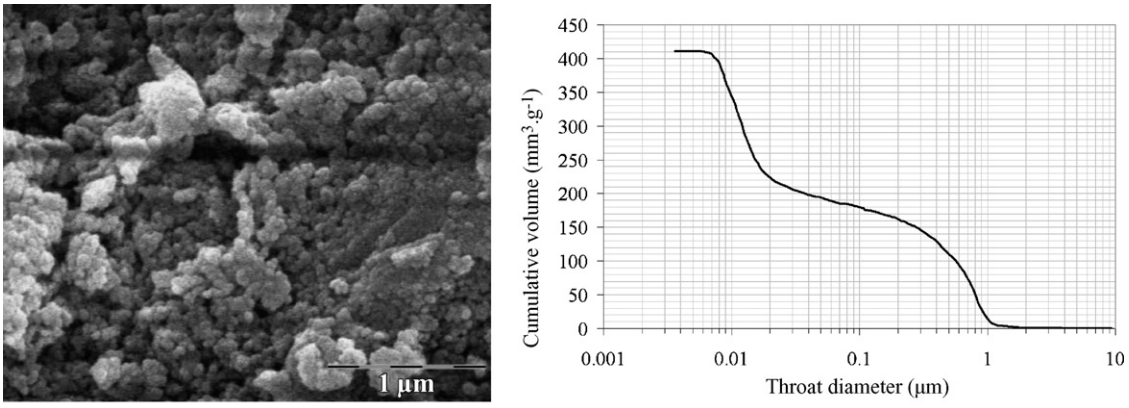

(a) (b)

Fig. 2. (a) Fracture of a sample containing 72% porosity and (b) the corresponding pore size distribution.

with diameter less than 50 nm and by macropores with diameter above 50 nm. The grain size of the zirconia particles increases from 62 to 70 nm when the applied thermal treatment at 750 °C is replaced by a thermal treatment at 1100 °C.

3.1.2. Alumina samples

Pore volume fractions were varied from 45 to 75% by adjusting v from 0.6 to 0.85. The micrograph in Fig. 3a reveals that the samples exhibit a more organised porous network. The mean

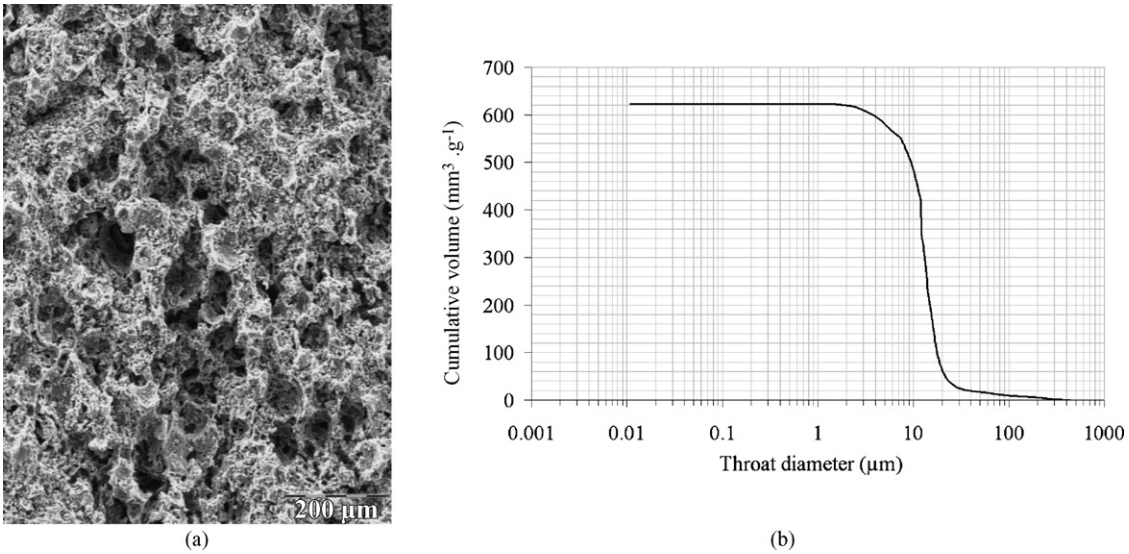

(a) (b)

Fig. 3. (a) Micrograph and (b) pore size distribution of an alumina sample containing 69% porosity.

Table 1
Adjusted values for the solid phase thermal conductivity by taking into account the interfacial thermal resistance of the grain boundaries

Material	$\lambda_{\text{single crystal}}$ ($W\,m^{-1}\,K^{-1}$)	Mean grain size (nm)	R^*_{int} ($m^2\,K\,W^{-1}$)	λ_{poly} ($W\,m^{-1}\,K^{-1}$)
8-YSZ	2.2	60–70	0.5×10^{-8}	1.9
Alumina	35	500	2×10^{-8}	15

grain size was then evaluated to be 0.5 μm. The micrograph and the intrusion curve of the mercury in the sample (Fig. 3b) are in agreement with a monomodal pore size distribution.

3.2. Thermal conductivity study

Table 1 presents the detailed calculation of the solid phase thermal conductivity for the zirconia and alumina samples.

3.2.1. Effect of the bimodal pore size distribution

Fig. 4 shows the measured effective thermal conductivity of the zirconia samples (λ_{eff}) as a function of pore volume fraction compared with the predictions made from the analytical models. Analytical theory based on isolated inclusions does not yield a good prediction of the effective thermal conductivity for such porous materials. In contrast experimental results can be seen to agree closely with predictions made with EMPT. The modelling with percolation theory can be improved even further, by taking into account a more detailed description of the microstructure, especially for porosity exceeding 65%.

Indeed EMPT considers a mixture of two homogeneous phases with a similar size of individual phase regions. Our porous samples are constituted by mesoporous and macroporous networks where the macropores are 100 times larger than the mesopores. An improvement to the modelling by EMPT can be achieved if we perform a two-step calculation. First, the thermal conductivity of the mixture constituted by the solid part and the mesoporous network is calculated. Second, the effective thermal conductivity of the sample is determined by using the previous calculated value and the volume of the macropores. Obviously, this method requires information on the pore size distribution of the sample to evaluate the respective proportions between V_{solid}, V_{mesopore} and $V_{\text{macropore}}$. In addition, two different values for the air thermal conductivity could be introduced with this two-step calculation to adjust λ_{air} with the pore size. The value calculated for $d = 10$ nm is used for the pore volume fraction corresponding to pores with diameter less than 50 nm (mesopores). The value obtained for $d = 1$ μm is assigned to the volume fraction of the macropores.

These final values calculated with EMPT, taking into account the bimodal pore size distribution and the Knudsen effect are compared with experimental results in Fig. 5. The agreement is now improved for porosity values exceeding 65%. EMPT calculations suggest also that the bimodal PSD give upper values for the effective thermal conductivity compared with a monomodal PSD.

Due to similar assumptions, computer simulations made on heterogeneous 3D geometrical structures (Fig. 1a) give values presented in Fig. 6 which are close to the EMPT predictions for a one-step calculation. The computer simulations made on the geometrical structures in Fig. 1b confirm that material with a bimodal PSD exhibits a greater effective thermal conductivity than a material with a monomodal PSD.

3.2.2. Effect of the microstructure organisation

EMPT gives values of the effective thermal conductivity which are very close to the experimental measurements for the

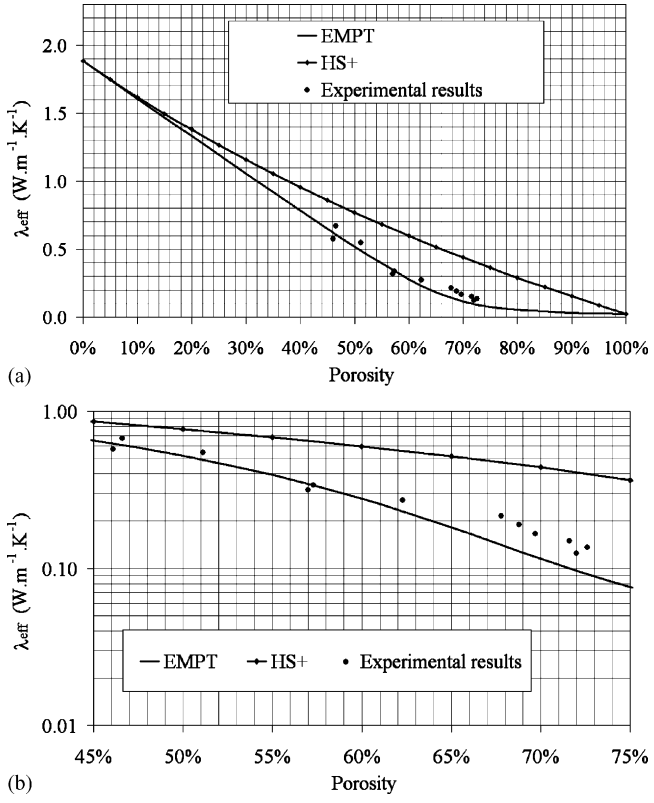

Fig. 4. Effective thermal conductivity of zirconia samples as a function of porosity for analytical predictions and experimental measurements. Calculation parameters: $\lambda_s = 1.9\ W\,m^{-1}\,K^{-1}$ and $\lambda_{\text{air}} = 0.026\ W\,m^{-1}\,K^{-1}$—(a) linear scale and (b) logarithm scale.

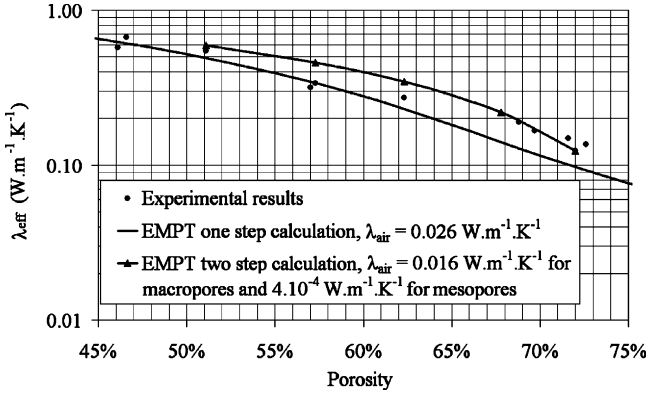

Fig. 5. Thermal conductivity of zirconia samples as a function of porosity for experimental measurements and EMPT calculations with and without taking into account the bimodal PSD and the Knudsen effect. Calculation parameters: $\lambda_s = 1.9\ W\,m^{-1}\,K^{-1}$ and λ_{air} on curve.

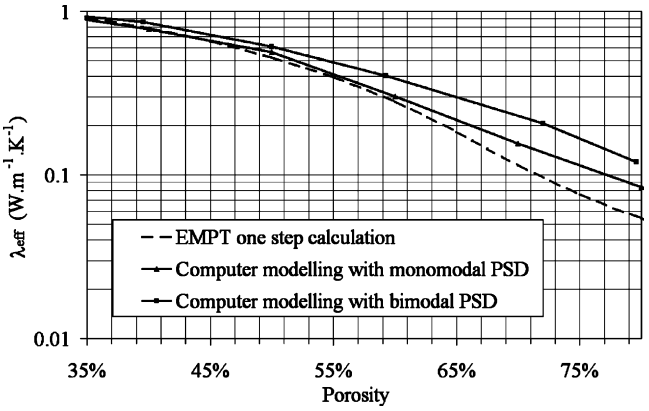

Fig. 6. Thermal conductivity as a function of porosity predicted by EMPT and FEM. Calculation parameters: $\lambda_s = 1.9\,W\,m^{-1}\,K^{-1}$ and $\lambda_{air} = 0.026\,W\,m^{-1}\,K^{-1}$.

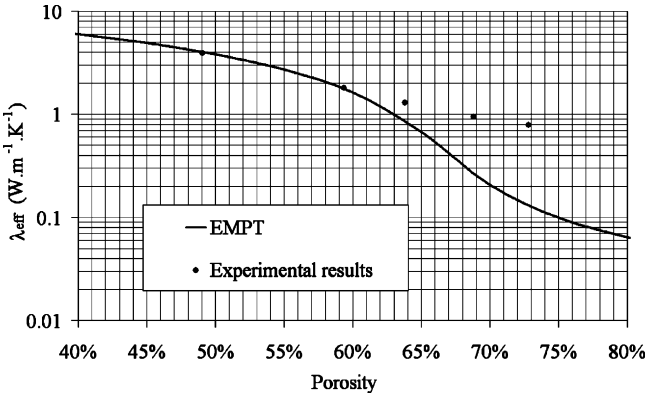

Fig. 8. Experimental measurements of thermal conductivity for alumina samples as a function of porosity compared to values calculated by EMPT. Calculation parameters: $\lambda_{solid} = 15\,W\,m^{-1}\,K^{-1}$ and $\lambda_{air} = 0.026\,W\,m^{-1}\,K^{-1}$.

zirconia samples. According to the percolation theory, applied to heat conduction, above the percolation threshold heat diffuses with more and more difficulty through the material and the effective thermal conductivity is governed by the gas phase. Indeed as shown in Fig. 7, the thermal conductivity curves calculated by EMPT as a function of porosity, for materials with a solid phase exhibiting different conductivity values, are very close above 70%. We can then deduce that, for obtaining a thermal insulating material by including greater than 70% porosity, the nature of the solid phase seems to be rather unimportant. Alumina samples were prepared in order to test this analytical prediction. Fig. 8 shows the measured effective thermal conductivity of the alumina samples (λ_{eff}) as a function of pore volume fraction and also the predictions made by EMPT. Compared with the analytical predictions, experimental values diverge strongly for porosity exceeding 65%. This behaviour could be explained by the more organised microstructure exhibited by the porous alumina, similar to a cellular solid. Indeed these alumina samples conserve more parallel solid paths to carry heat, compared with a heterogeneous material, and consequently the effective thermal conductivity values are high in comparison with predictions made with EMPT.

Computer calculations made on the geometrical structures presented in Fig. 1c, which exhibit a perfectly organised

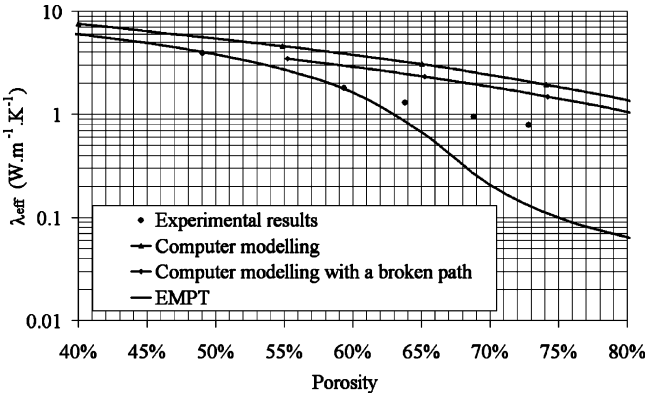

Fig. 9. Effective thermal conductivity of alumina samples as a function of porosity calculated by FEM for comparison to experimental measurements. Calculation parameters: $\lambda_s = 15\,W\,m^{-1}\,K^{-1}$ and $\lambda_{air} = 0.026\,W\,m^{-1}\,K^{-1}$.

open porosity, give values for the effective thermal conductivity which present a similar behaviour to the experimental measurements (Fig. 9). Obviously, these geometrical models overestimate the effective thermal conductivity due to the

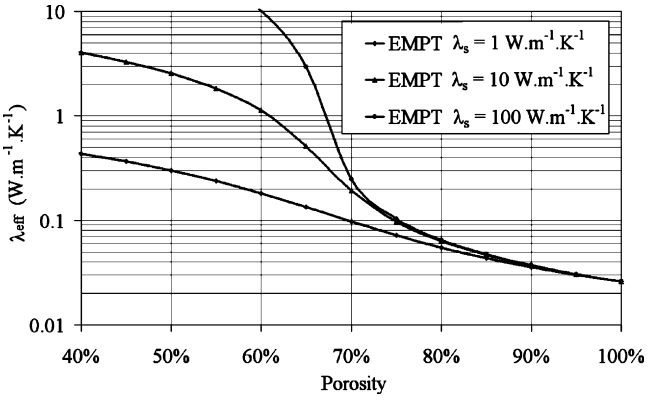

Fig. 7. Thermal conductivity as a function of porosity calculated by EMPT for $\lambda_s = 1$, 10 and 100 $W\,m^{-1}\,K^{-1}$ and $\lambda_{air} = 0.026\,W\,m^{-1}\,K^{-1}$.

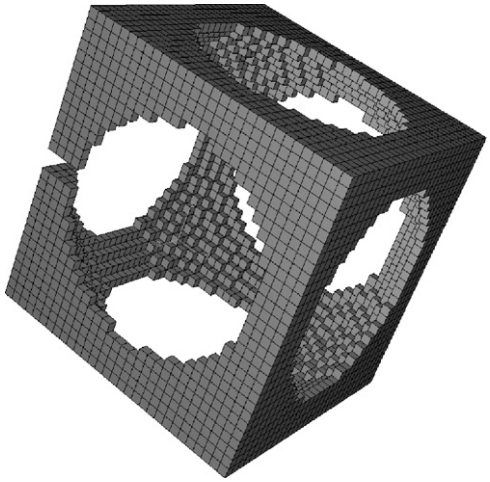

Fig. 10. Organised geometrical model with a broken path in the heat flow direction.

perfect microstructure. More realistic geometries were studied by damaging available paths for heat conduction as shown in Fig. 10. As a result, the predicted thermal conductivity values plotted in Fig. 9 decrease and approach the experimental results.

4. Conclusion

The prediction of the effective thermal conductivity of a material with a large pore volume fraction required a detailed description of the porous network. Obviously, the thermal conductivity is directly affected by the pore volume fraction. But it has been shown that the pore size distribution and also the microstructure organisation strongly influence the effective thermal conductivity. The thermal conductivity of the most porous zirconia samples approaches a lower limit of $0.1\,W\,m^{-1}\,K^{-1}$.

According to these results, a very thermally insulating material should exhibit a large pore volume fraction. These pores should be as fine as possible with a monomodal size distribution and not spatially organised. Porous zirconia samples with a perfect cellular arrangement were prepared recently following a hetero-coagulation strategy. The measured effective thermal conductivity gives values significantly above the EMPT predictions. This confirms the results obtained for the semi-organised alumina samples. In the case of a cellular solid, the effect of a bimodal PSD on the effective thermal conductivity remains to be investigated.

Acknowledgement

Benoît Naït-Ali would like to thank the French Ministry of Research and Technology for the Ph.D. study grant.

References

1. Schulle, W. and Schlegel, E., Fundamentals and properties of refractory thermal insulating materials (high-temperature insulating materials). *Ceramic Monographs—Handbook of Ceramics*, *Supplement to Interceram* 1991, **40**(7), No. 2.6.3.
2. Litovsky, E., Shapiro, M. and Shavit, A., Gas pressure and temperature dependances of thermal conductivity of porous materials. Part 2. Refractories and ceramics with porosity exceeding 30%. *J. Am. Ceram. Soc.*, 1996, **79**, 1366–1376.
3. Grandjean, S., Absi, J. and Smith, D.S., Numerical calculation of the thermal conductivity of porous ceramics based on micrographs. *J. Eur. Ceram. Soc.*, in press, doi:10.1016/j.jeurceramsoc.2005.07.061 (corrected proof, available online 12 September 2005).
4. Collishaw, P. G. and Evans, J. R. G., An assessment of expressions for the apparent thermal conductivity of cellular materials. *J. Mater. Sci.*, 1994, **29**, 2261–2273.
5. Bucko, M. M. and Haberko, K., Crystallization of zirconia under hydrothermal conditions. *J. Am. Ceram. Soc.*, 1995, **78**, 3397–3400.
6. Degiovanni, A., Diffusivité et méthode Flash. *Rev. Gén. Therm. (France)*, 1977, **185**, 420–441.
7. Raghavan, S., Wang, H., Dinwiddie, R. B. and Porter, W. D., The effect of grain size, porosity and yttria content on the thermal conductivity of nanocrystalline zirconia. *Scripta Mater.*, 1998, **39**, 1119–1125.
8. Weast, R. C., ed., *Handbook of Chemistry and Physics*. 55th ed. CRC Press, Cleveland, Ohio, 1974, p. E2.
9. Yang, H. S., Bai, G. R., Thompson, L. J. and Eastman, J. A., Interfacial thermal resistance in nanocrystalline yttria stabilised zirconia. *Acta Mater.*, 2002, **50**, 2309–2317.
10. Smith, D. S., Fayette, S., Grandjean, S., Martin, C., Telle, R. and Tonnessen, T., Thermal resistance of grain boundaries in alumina ceramics and refractories. *J. Am. Ceram. Soc.*, 2003, **86**, 105–111.
11. Hashin, Z. and Shtrikman, S., A variational approach to the theory of the effective magnetic permeability of multiphase materials. *J. Appl. Phys.*, 1962, **33**, 3125–3131.
12. Landauer, R., The electrical resistance of binary metallic mixtures. *J. Appl. Phys.*, 1952, **21**, 779–784.
13. Ast, D. G., Evidence for percolation-controlled conductivity in amorphous As_xTe_{1-x} films. *Phys. Rev. Lett.*, 1974, **33**, 1042–1045.